Adenoviral Transduction of *TESTIN* Gene into Breast and Uterine Cancer Cell Lines Promotes Apoptosis and Tumor Reduction *In vivo*

Manuela Sarti,[1] Cinzia Sevignani,[1] George A. Calin,[1] Rami Aqeilan,[1] Masayoshi Shimizu,[1] Francesca Pentimalli,[1] Maria Cristina Picchio,[1] Andrew Godwin,[2] Anne Rosenberg,[3] Alessandra Drusco,[1] Massimo Negrini,[4] and Carlo M. Croce[1]

[1]Kimmel Cancer Center, Jefferson Medical College of Thomas Jefferson University; [2]Fox Chase Cancer Center, Philadelphia, Pennsylvania; [3]Thomas Jefferson University Hospital, Philadephia, PA; and [4]Centro Interdipartimentale per la Ricerca sul Cancro, Dipartimento di Medicina Sperimentale e Diagnostica, Universita' degli Studi di Ferrara, Ferrara, Italy

ABSTRACT

Purpose: **The human *TESTIN* (*TES*) gene is a putative tumor suppressor gene in the fragile chromosomal region *FRA7G* at 7q31.1/2 that was reported to be altered in leukemia and lymphoma cell lines. In this report, we investigated the effect of *TES* gene expression *in vivo* to evaluate a possible role of *TES* gene in human cancer.**

Experimental Design: **We have analyzed the expression of *TES* gene in a panel of 25 breast tumors and 17 cell lines of breast, colon, and uterine cancers. Furthermore, to evaluate the potential of *TES* gene therapy, we studied the effects of adenoviral *TES* transduction (Ad-*TES*) in cell lines with undetectable *TES* expression (T47D and MES-SA) as well as in MCF-7 cell line where *TES* expression is normal.**

Results: **Twenty-five percent of primary breast tumor samples as well as the breast cancer cell line T47D and the uterine sarcoma cell line MES-SA were negative or displayed low levels of *TES*. After *TES* restoration by Ad-*TES* transduction, T47D and MES-SA cell lines underwent apoptosis. Furthermore, *TES* expression significantly reduced the tumorigenic potential of both T47D and MES-SA in nude mice, whereas the untreated cells and Ad-GFP-infected cells showed tumor growth *in vivo*. The *TES*-positive cell line control (MCF-7) was not affected by TES expression and did not show a reduction of tumorigenicity in nude mice after infection with Ad-*TES*.**

Conclusions: **Ad-*TES* expression inhibit the growth of breast and uterine cancer cells lacking of *TES* expression through caspase-dependent and caspase-independent apoptosis, respectively, suggesting that Ad-*TES* infection should be explored as a therapeutic strategy.**

Received 1/27/04; revised 8/25/04; accepted 9/13/04.
Grant support: United State Public Health Service grants CA 77738 and CA56336 from the National Cancer Institute.
The costs of publication of this article were defrayed in part by the payment of page charges. This article must therefore be hereby marked *advertisement* in accordance with 18 U.S.C. Section 1734 solely to indicate this fact.
Note: M. Sarti and C. Sevignani contributed equally to this work.
Requests for reprints: Carlo M. Croce, Comprehensive Cancer Center, Ohio State University, Wiseman Hall, Room 445D, 400 West 12th Avenue, Columbus, OH 43210. E-mail: Carlo.Croce@osumc.edu.

INTRODUCTION

Fragile sites may play a role in both loss of tumor suppressor genes and amplification of oncogenes. The human *TESTIN* gene (*TES*) is in the fragile chromosomal region *FRA7G* at 7q31.1/2. *FRA7G* is a locus that shows loss of heterozygosity in many human malignancies, and some studies suggest that one or more tumor suppressor genes involved in multiple malignancies are in this region (1, 2). *FRA7G* has been previously localized between marker D7S486 and a marker within the *MET* gene, MetH (3). This region is known to encompass several genes, including two putative tumor suppressor genes, *caveolin-1* and *TES* (1, 4), as well as *caveolin-2* (5) and the *MET* proto-oncogene (6).

TES is widely expressed in all normal human tissues. Lack of *TES* mRNA expression was found in several cancer-derived cell lines, particularly hematopoietic, breast, and ovarian cancer cell lines, as well as in primary tumors (1) and was correlated with methylation of the *TES* CpG island (1, 2). A forced overexpression of *TES* resulted in growth reduction of Ovcar5 (ovarian) and HeLa (cervical) carcinoma cell lines (2), indicating that *TES*, as a putative tumor suppressor gene, can be a negative regulator of cell growth (2). However, the function of *TES* is currently unknown and is predicted to encode a highly conserved protein of 421 amino acids containing three COOH-terminal LIM domains that seem to be important for focal adhesion targeting (7).

Here, we present molecular and functional data supporting the involvement of *TES* gene in breast and uterine tumorigenesis. In particular, we investigated the effects of TES protein expression in TES-negative and TES-positive breast carcinoma cell lines (T47D and MCF-7, respectively) and in TES-negative uterine sarcoma cells (MES-SA) by an adenoviral vector. We now show by investigating cell proliferation, cell cycle profiles, and tumorigenicity that the Ad-*TES*-transduced cell lines T47D and MES-SA show impaired cell proliferation *in vitro* and a reduced ability to form tumors in nude mice.

MATERIALS AND METHODS

Patient Samples and Cell Lines. We used 25 primary breast tumors obtained from University of Ferrara (17 samples) and from Fox Chase Cancer Center (8 samples). The tumor stage was known for 17 of 25 (12 were ductal carcinomas in stage II and III, 4 adenocarcinomas in stage II and III, and 1 colloid carcinoma in stage II) as well as the presence or absence of hormonal receptors. Samples were collected according to the

institutional protocols. Total RNA was extracted with RNAwiz reagent (Ambion, Inc., Austin, TX) following the manufacturer's instructions, and reverse transcription was carried out using SuperScript First-Strand Synthesis System (Invitrogen-Life Technologies, Carlsbad, CA). The breast cancer cell lines MCF-7, T47D, MDA-MB-436, MDA-MB-231, and SKbr-3, the uterine sarcoma cell line MES-SA, and the colon cancer cell lines WIDR, LoVo, LS411, LS513, LS1034, SN4C2B, HT-29, HCT-116, SW480, and SW620 were obtained from American Type Culture Collection (Manassas, VA) and cultured as indicated. 293 cells were purchased from Qbiogene (Carlsbad, CA), cultured in DMEM and 10% fetal bovine serum, and used for packaging, expanding, and titration of adenoviral vectors.

PCR and Reverse Transcription-PCR. All the primary breast tumors and cell lines were studied for *TES* expression by reverse transcription-PCR. As controls, we used breast, uterus, and colon normal RNA (Ambion). The conditions of PCR reaction were 95°C for 3 minutes then 30 cycles at 94°C for 30 seconds, 58°C for 30 seconds, and 72°C for 30 seconds then 72°C for 10 minutes using the following primers: *TES2* INT forward 5′-CCTTCAAAGTGCCATGAGTTGTCTC-3′ and *TES2* INT reverse 5′-TTCATACTCAGTTTGCAGCAA-TAGC-3′. The specific product was 241 bp long.

Recombinant Adenoviral Vector and *In vitro* Transduction. The Ad-*TES2* vector was prepared according to the manufacturer's instructions (Qbiogene). The full-length TES (isoform 2, TES2) cDNA was isolated from normal human liver DNA (Clontech, Palo Alto, CA) by PCR strategy, cloned into an Adenovator-CMV5-IRES-GFP transfer vector, and confirmed by DNA sequencing (1). In this vector, green fluorescent protein (GFP) is coexpressed with *TES* gene in an internal ribosome entry site expression cassette, and both are placed under the control of a cytomegalovirus promoter/enhancer (CMV5). The recombinant adenoviral vector plasmid Ad-*TES2* was transfected into human fetal kidney 293 cells (Qbiogene); after 14 to 21 days, homologous recombination occurred in cells, leading to plaque formation. Plaques were isolated, and supernatants were eluted to infected 293 cells in 24-well culture plates. After selection of viral clones, 293 cells were infected with individual clones to develop virus stocks. An Ad-GFP vector was used as a control (Qbiogene). Viral vectors were amplified in 293 cells and purified by CsCl gradient centrifugation. Viral titers were determined by assay for plaque-forming units. Cells (1×10^6 per well for 6-well plates, 5×10^5 per well for 12-well plates, and 1×10^5 cells per well for 48-well plates) were transduced with adenoviral vectors by directly applying the diluted viruses into the growth medium at different multiplicity of infections (MOI). The transduction efficiency was determined by direct visualization using fluorescent microscopy of GFP-expressing cells after Ad-GFP infection. The transgene expression was detected by reverse transcription-PCR and by anti-GFP and anti-TES antisera by Western blotting.

Immunoblot Analysis. Immunoblot analysis was done by standard protocols (8). Briefly, 5×10^5 cells were cultured in 60 mm diameter dishes and lysed on ice in 300 μl of lysis buffer. Protein lysates were loaded on 4% to 20% linear gradient SDS-PAGE gels and electroblotted to polyvinylidene difluoride membranes (Amersham Pharmacia Biotech, Piscataway, NJ). The membranes were blocked with 5% skim milk and incubated with the indicated antisera. After reaction with an appropriate secondary antiserum, the immunoreactive bands were detected by the enhanced chemiluminescence system (Amersham Pharmacia Biotech) according to the manufacturer's protocol. For Western blot analysis, we used the following antisera and concentrations: rabbit polyclonal anti-TES at 1:1,000 (Zymed, South San Francisco, CA), mouse monoclonal anti-caspase-2 at 1:1,000 (BD Biosciences, San Jose, CA), mouse monoclonal anti-caspase-3 at 1:500 (BD PharMingen, San Diego, CA), rabbit polyclonal anti-caspase-8 at 1:250 (Chemicon, Temecula, CA), rabbit polyclonal anti-caspase-9 at 1:200 (Santa Cruz Biotechnology, Santa Cruz, CA), rabbit polyclonal anti–poly(ADP-ribose)polymerase at 1:1,000 (Upstate, Charlottesville, VA), and, only for MES-SA cell line, rabbit polyclonal anti–apoptotic protease activating factor-1 at 1:500 (BD PharMingen), mouse monoclonal anti-Bcl-2 at 1:1,000 (BD Biosciences), mouse monoclonal anti-caspase-7 at 1:1,000 (BD PharMingen), mouse monoclonal anti- cytochrome *c* at 1:500 (BD PharMingen), rabbit polyclonal anti–apoptosis-inducing factor (AIF) at 1:1,000 (BD PharMingen), rabbit polyclonal anti-survivin at 1:1,000 (Novus Biologicals, Littleton, CO), and anti-actin at 1:3,000 (Sigma Chemical Co., San Louis, MO).

Cell Growth and Flow Cytometry. For growth curves, 1×10^5 cells (T47D, MCF-7, and MES-SA) were cultured in T-25 cm^2 tissue culture flasks and infected using appropriate MOIs for each of the three cancer cell lines analyzed and counted everyday for 1 week. The number of viable cells per well was determined at indicated times in triplicate, excluding the dead cells by trypan blue staining. For flow cytometry analysis, 5×10^5 cells were seeded in 60 mm dishes; infections were at MOI 50 and 100 on each cell line; cells were harvested after 72, 120, and 144 hours for T47D and MCF-7 and after 72, 120, 144, and 168 hours for MES-SA; washed in PBS; fixed in cold methanol; incubated in RNase; and stained with propidium iodide (50 μg/mL). Cells were then analyzed for DNA content as a function of cell number as described (9). The samples were examined by flow cytometry on an EPICS-XL scan (Beckman-Coulter, Fullerton, CA) using doublet discrimination gating.

DNA Fragmentation Analysis in MES-SA Cell Line. For DNA preparation, 1×10^5 cells were seeded in six-well plates and infected with Ad-*TES2* and Ad-GFP at MOI 100; concurrently, we incubated a control culture without infection. Cells (0.5×10^6 to 1×10^6) were harvested after 168 hours and processed according to a standard protocol (Chemicon).

***In vivo* Tumorigenicity.** Animal studies were repeated twice and performed according to institutional guidelines. The MCF-7 and T47D breast cancer cell lines and MES-SA uterine sarcoma cell line were plated and infected *in vitro* under three conditions (Ad-*TES2*, Ad-GFP, and mock) at MOI of 100. Forty-eight hours after infection, 5×10^6 T47D and MCF-7 and 3×10^6 MES-SA viable cells suspended in 500 μL PBS were injected s.c. into the left and right flanks and back of 6-week-old female *nu/nu* mice (Charles River, Cambridge, MA). For MES-SA cell line, 12 mice per group treated with infected cells and 16 mice for the mock group; for T47D cell lines, 11 mice for the group treated with Ad-GFP-infected cells, 6 mice for the group treated with Ad-*TES2*-infected cells, and 9 mice for the mock

group; for MCF-7, 4 mice per group treated with infected cells and 13 mice for the mock group. MCF-7 and T47D are estrogen receptor–positive cell lines and require estrogens for tumorigenesis *in vivo* (10, 11). Conjugated estrogens (Premarin, Ayerst Laboratories, Philadelphia, PA) were injected i.p. at 15 mg/kg body weight before injection of tumor cells and a day per week. The tumor diameters for MCF-7 and T47D cell injection, were monitored weekly for at least 3 months or until death and for 3 weeks for MES-SA cells. The tumor volume was calculated using the formula: length × width / 4 × π. All tumors were weighed after necropsy at the end of each experiment, fixed in formalin, and embedded in paraffin.

Statistics. Both *in vivo* and *in vitro* results were expressed as mean ± SD or mean ± SE. Student's two-sided *t* test was used to compare the values of the test and control samples. $P < 0.05$ was taken as significant.

RESULTS

TES Expression Is Reduced in Breast Tumors and in Breast Cancer Cell Line T47D and in MES-SA Uterine Sarcoma Cell Line

When 25 primary breast tumor samples were studied and compared with a normal breast tissue (Ambion), we found reduced signal of *TES* mRNA in 9 (36%) samples (Fig. 1*A*). Analysis for the expression of endogenous TES protein in breast cancer cell lines and an uterine sarcoma cell line showed that endogenous TES protein was undetectable in T47D and MES-SA cell lines compared with normal breast and uterine cells (data not shown). MCF-7, MDA-MB-436, MDA-MB-231, and Skbr-3 cells (data not shown) and all the colon cancer cell lines analyzed expressed normal levels of endogenous *TES* mRNA (Fig. 1*C*) and protein (data not shown) compared with the normal samples. We chose the breast carcinoma cell line MCF-7 as a *TES*-positive control to verify the effects of adenoviral transfection of *TES* gene. Previous Northern blots on breast cancer cell lines showed that T47D has an undetectable expression of *TES* gene (1).

Ad-*TES* Expression in Cancer Cell Lines *In vitro*

T47D, MCF-7, and MES-SA were infected with either Ad-*TES2* or Ad-GFP. After 72 and 168 hours of infection, reverse transcription-PCR showed *TES* expression in *TES*-negative cell lines (Fig. 1*C*), and the immunoblot analysis showed *TES* transgene overexpression in all Ad-*TES2*-transduced cells. The infection levels for T47D were ~20% to 30% at MOI 20, 70% to 75% at MOI 50, and 90% to 95% at MOI 100; for MCF-7 ~20% at MOI 20, 70% at MOI 50, and 80% to 85% at MOI 100; and for MES-SA ~25% at MOI 20, 80% at MOI 50, and 95% at MOI 100. Therefore, we decided to conduct the experiments using MOI 50 and 100 for all three cell lines.

Cell Growth Analysis of Ad-*TES2*-Infected Breast Cancer and Uterine Sarcoma Cells *In vitro*

For growth kinetics curves, 1×10^5 cells were cultured in T-25 cm^2 tissue culture flasks and infected using appropriate MOIs. Cell counts obtained from triplicate experiments revealed that *in vitro* growth of Ad-*TES2*-infected cells (T47D and MES-SA) was significantly inhibited compared with Ad-GFP-infected cells (Fig. 2*A* and *B*). The Ad-*TES2*-infected MCF-7 cells grew as well as the Ad-GFP controls (Fig. 2*C*). Statistically significant

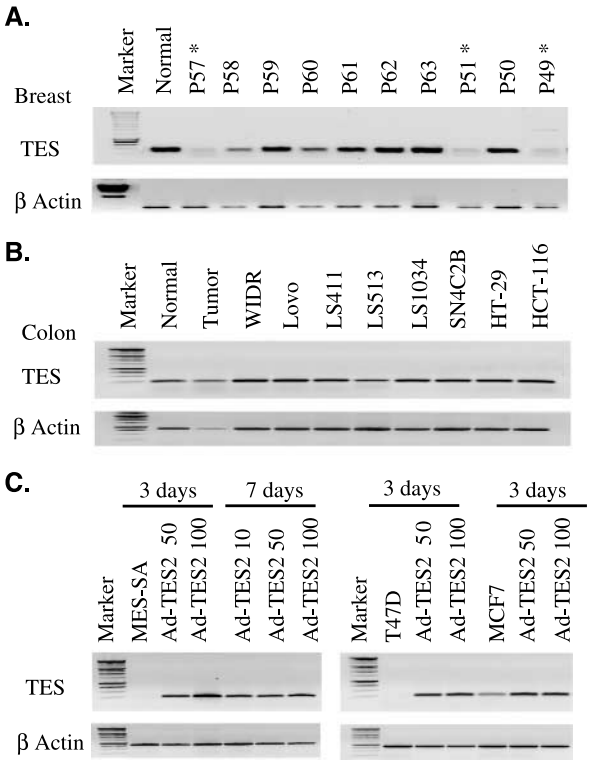

Fig. 1 Reverse transcription-PCR expression of *TES* in breast tumors and cancer-derived cell lines. *A,* breast tumor samples; *B,* colon cell lines; *C,* T47D, MES-SA, and MCF-7 cell lines, wild type (untreated) and Ad-*TES2*-infected. Asterisks, samples with low expression.

differences were observed in cell growth for Ad-*TES2* and Ad-GFP infection at a range of MOIs in T47D and MES-SA ($P < 0.03$ for each), whereas no significant difference in MCF-7 cell line was found ($P = 0.08$).

Cell Cycle Analysis and Apoptosis of Ad-*TES2*-Infected Cancer Cell Lines

To study cell cycle alterations induced by *TES* overexpression, each cell line was infected at several MOIs with either Ad-*TES2* or Ad-GFP. A sub-G_1 cell population was observed after Ad-*TES2* transduction in T47D and MES-SA, whereas no modifications in cell cycle profile were detected in MCF-7 cell line and after infection with Ad-GFP. One hundred twenty hours after infection with Ad-*TES2* (MOI 100), 31.20% of T47D cells were in the sub-G_1 fraction, whereas 168 hours after infection (MOI 100), 38% of MES-SA cells were dead (Fig. 3). *TES* induction of cell death was MOI and time dependent. Therefore, Ad-*TES2* infection induces high levels of apoptosis in cells negative for *TES*.

Analysis of the Apoptotic Pathways in *TES*-Reexpressing Cells

T47D, MCF-7, and MES-SA cancer cell lines were infected with increasing MOIs, and the fraction of transduced cells was monitored by confocal microscopy and fluorescence-activated cell sorting analysis. To exclude virus-specific effects, we compared cell lysates and mRNA extracted from cells infected with Ad-GFP at the same MOI. To investigate the

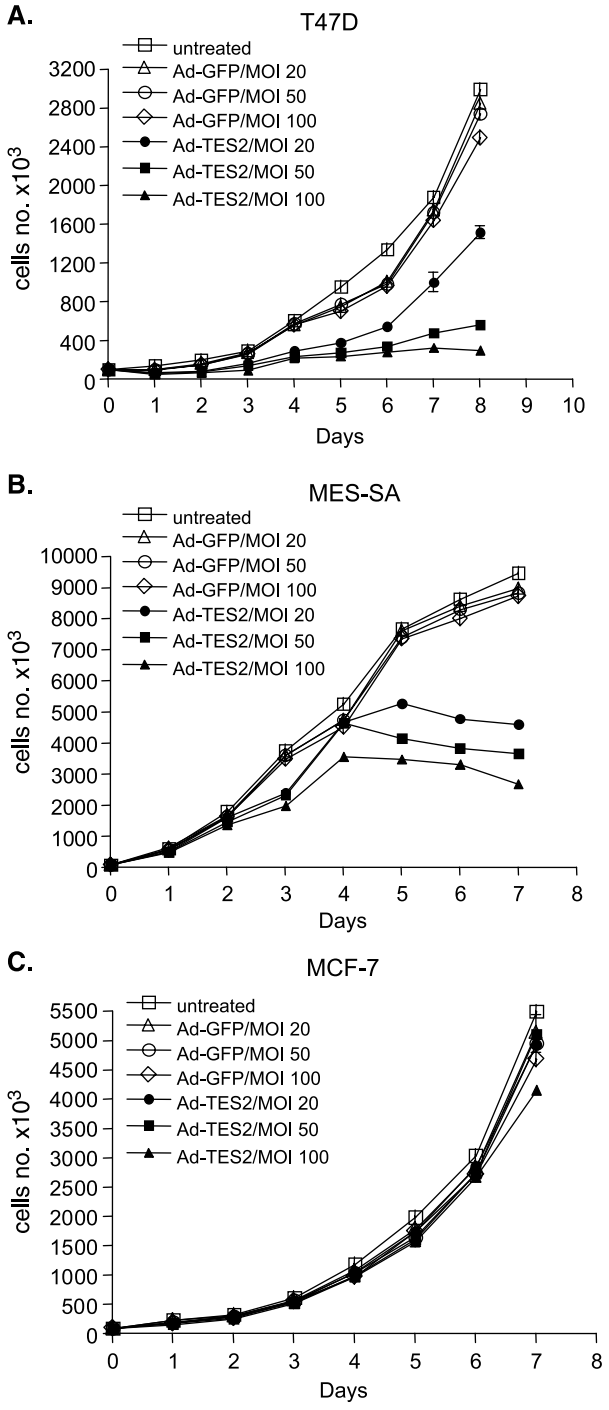

Fig. 2 Proliferation analysis of Ad-*TES*-infected breast cancer and uterine sarcoma cells *in vitro* (*A*-*C*). Growth rate was assessed by cell counting as described in MATERIALS AND METHODS. Points, total cell number; bars, SD. Representative of mean of triplicate experiments. Statistically significant differences were observed in cell growth for Ad-*TES2* and Ad-GFP infection at a range of MOIs in T47D and MES-SA ($P < 0.03$; *A* and *B*), whereas no significant difference in MCF-7 cell line was shown ($P = 0.08$; *C*).

molecular mechanism of the oncosuppressive activity of Ad-*TES2*, the expression of molecules involved in the apoptotic cascade was assessed, such as Bcl-2, apoptotic protease activating factor-1, caspase-2, caspase-3, caspase-7, caspase-8, caspase-9, and poly(ADP-ribose)polymerase-1. In the T47D cell line, pro-caspase-3, pro-caspase-8, and pro-caspase-9 levels were reduced in Ad-*TES2*-infected cells with respect to Ad-GFP-infected cells, demonstrating the activation of intrinsic and extrinsic apoptosis pathways (Fig. 4*A*). No variations in caspases and poly(ADP-ribose)polymerase levels were detected in uninfected and Ad-GFP- and *TES2*-infected MCF-7 cells, demonstrating that the infection with *TES* in a cell line with normal expression of this gene has no effect on the main mediators of apoptosis (Fig. 4*B*). MCF-7 cells did not show expression of pro-caspase-3 (data not shown), because they do not constitutively express caspase-3 (12, 13). In Ad-*TES2*-infected MES-SA cells, we found normal levels of Bcl-2, apoptotic protease activating factor-1, caspases, and poly(ADP-ribose)polymerase, and cytochrome *c* was not released (data not shown). We observed DNA fragmentation (data not shown), down-regulation of survivin, and successive overexpression of AIF with respect to Ad-GFP-infected cells and untreaded cells (Fig. 4*C*). These data confirm that the main role of survivin is in cell cycle progression and that low levels or the inhibition of this protein are sufficient to induce cell death (14). Moreover, it is important for the antagonistic relationship between survivin and AIF in caspase-independent pathway to enhance the apoptotic mechanism (15, 16).

Tumorigenicity of Adenoviral-Infected Breast Cancer and Uterine Sarcoma Cell Lines *In vivo*

When nude mice were s.c. inoculated with T47D and MCF-7, cells were tumorigenic only when mice were treated with estrogens (10), whereas MES-SA produced large tumors, in concordance with published information (Table 1). We tested the tumorigenic potential of Ad-*TES2*-infected T47D, MCF-7, and MES-SA cells in three groups of mice (Fig. 5). In the first group, mice were injected with 5×10^6 T47D viable cells that had been infected *in vitro* at MOI 100 with Ad-*TES2* (6 mice) or with Ad-GFP (11 mice) or mock (9 mice) and cultured for 48 hours before injection. Tumor growth was suppressed in 84% of mice injected with Ad-*TES2*-infected T47D cells (average tumor weight at the end of the experiment was 0.013 ± 0.006 versus 0.014 ± 0.010 versus 0.001 ± 0.003 g for mock infection, Ad-GFP-infected, Ad-*TES2*-infected cells, respectively; Fig. 5*B*). In the second group, mice were injected with 5×10^6 MCF-7 viable cells that had been infected at MOI 100 with Ad-*TES2* (4 mice) or with Ad-GFP (4 mice) or mock (13 mice) and cultured for 48 hours before injection. In the third group, mice were injected with 3×10^6 MES-SA viable cells that had been infected at MOI 100 with Ad-*TES2* (12 mice) or with Ad-GFP (12 mice) or mock (16 mice) and cultured for 48 hours before injection. Tumor growth of MES-SA was suppressed in 75% of mice injected with Ad-*TES2*-infected cells (average tumor weight at the end of the experiment was 0.405 ± 0.475 versus 0.399 ± 0.436 versus 0.0275 ± 0.057 g for mock infection, Ad-GFP-infected, Ad-*TES2*-infected cells, respectively; Fig. 5*A*). Therefore, Ad-*TES2* infection has a significant effect of tumor reduction *in vivo* in cells negative for *TES*. In contrast, we did

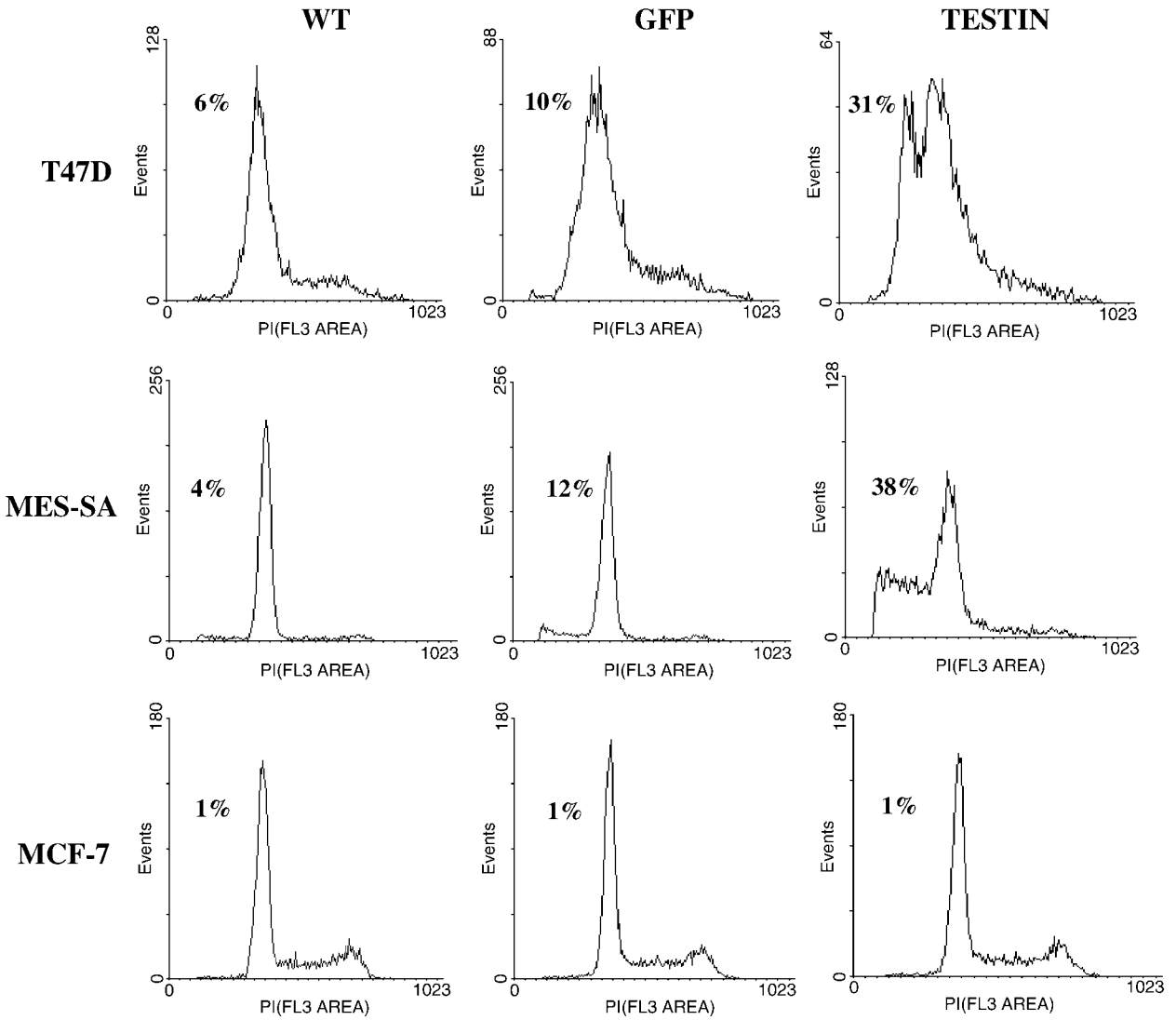

Fig. 3 FACScan analysis of cell cycle. Sub-G_1 content of *TES2*-infected breast and uterine cancer cell lines. Cells were infected with 100 MOI of Ad-GFP or Ad-*TES2* for 5 days (T47D and MCF-7) and for 7 days (MES-SA) and then fluorescence-activated cell sorting analyzed for DNA content as a function of cell number using propidium iodide. Numbers, percentage of cells in sub-G_1 phase (i.e., apoptotic cells).

Table 1 Cancer cell line characteristics

Cell line	Histotype	*In vivo* tumorigenicity	*TES* status Western blot	Transduction levels, % (MOI)
T47D	Ductal breast carcinoma	Low	Negative	30 (20) 75 (50) 95 (100)
MCF-7	Breast adenocarcinoma	Low	Positive	20 (20) 70 (50) 85 (100)
MES-SA	Uterine sarcoma	High	Negative	25 (20) 80 (50) 95 (100)

not observe significant differences in growth of tumors derived from MCF-7 untreated cells and infected with Ad-GFP or Ad-*TES2* (average tumor weight at the end of the experiment was 0.02 ± 0.017 versus 0.005 ± 0.010 versus 0.006 ± 0.007 g for mock infection, Ad-GFP-infected, Ad-*TES2*-infected cells, respectively; data not shown).

DISCUSSION

The human *TES* gene is located at 7q31.1/2 within the fragile chromosomal region *FRA7G* that has been reported to be involved in loss of heterozygosity in several human tumors (1, 2). Northern blot analysis, reverse transcription-PCR analysis, and DNA methylation profiles show that *TES* is not expressed in a variety of tumor cell lines, particularly hematopoietic, breast, and ovarian cancer cell lines, as well as primary tumors (1, 2). Therefore, *TES* was proposed as a tumor suppressor mainly inactivated by promoter hypermethylation. In this study, we evaluated the possible role of *TES* gene therapy for complementary cancer treatment in human cancers lacking of *TES* expression. As a first step, we evaluated the *TES* expression in breast samples as well as various cancer cell lines, including an uterine cell line. Breast cancer is among the most common human cancers, representing 32% of all cancers in the United States, and it is a leading cause of death for American women (17). Uterine sarcoma is a highly aggressive malignant neoplasm with early lymphatic and hematogenous spread; the mean age is 58 years, and 5-year survival is between 38% and 45% (18, 19). Despite important advances in chemotherapy, radiotherapy, and surgery, complementary therapeutic strategies should be considered for improving the outcome of the patients with these types of tumors.

We analyzed the expression of *TES* gene in 25 primary breast tumor samples and we found reduced expression in 9 (36%) samples; also, in 1 of 10 breast cancer derived cell lines, the TES protein was completely absent, consistent with reports of *TES* expression loss in breast cancer (1, 20). We found also an undetectable expression in a uterine sarcoma cell line (MES-SA). Adenoviral transduction of the *TES* gene product in two breast cancer cell lines (T47D and MCF-7) and in the uterine sarcoma cell line (MES-SA) caused suppression of cell growth and alterations in cell cycle only in cells negative for *TES* (T47D and MES-SA). Toxicity of the viral vector was ruled out, because the control virus, Ad-GFP, did not cause the same alterations. Similar antiproliferative effects have been observed in other two tumor cell lines transfected with *TES* expression constructs, Ovcar5 (ovarian carcinoma) and HeLa (cervical carcinoma; ref. 2), suggesting the *TES* gene therapy may be useful for treatment of various cancers. Ad-*TES* expression barely affected cell cycle and cell growth in MCF-7 cells in which the gene was abundantly expressed.

Furthermore, this study shows evidence of efficient suppression of *in vivo* tumorigenicity of breast and uterine cancer cell lines by adenovirus transducing the *TES* gene. A possible role for *TES* in gene therapy is supported by results of experiments after injection of nude mice with *TES*-transduced breast and uterine cancer cells. The tumorigenicity of MES-SA cells was significantly reduced by Ad-*TES* treatment; a similar result was found for T47D cells supplemented with estrogens, whereas no significant reduction of tumorigenicity was observed in animals treated by estrogens and injected with *TES*-transduced MCF-7 cells.

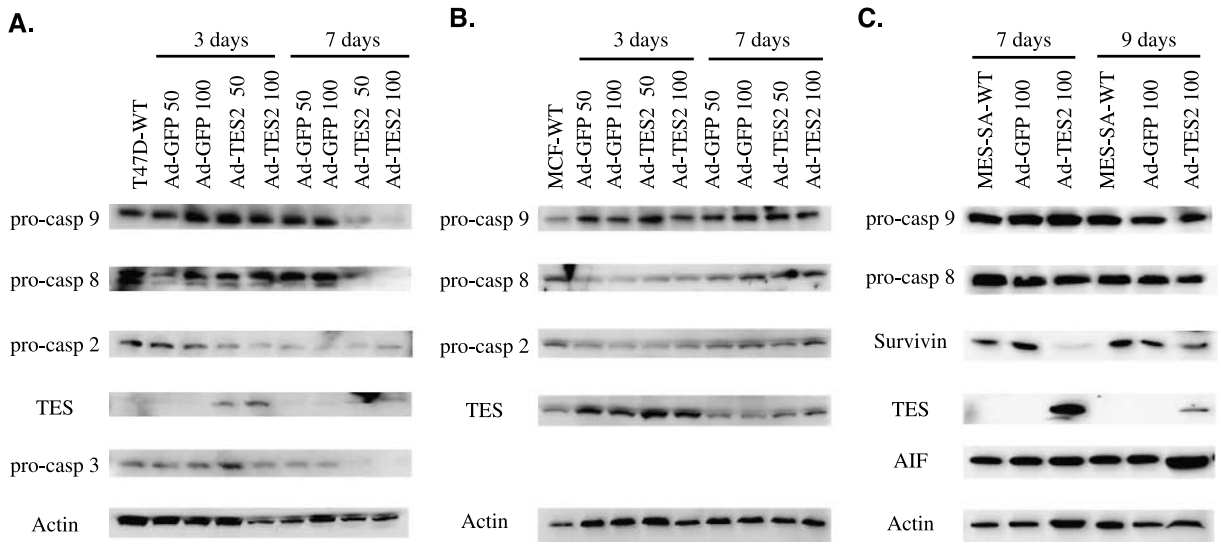

Fig. 4 Modulation of apoptosis-related proteins in Ad-*TES2*-infected cells. *A,* T47D cells: Caspase-9 activation shown as a reduction of the 35-kDa band of the pro-caspase-9 was pronounced in infected cells. Pro-caspase-3 and pro-caspase-8 expression was significantly affected by exogenous *TES* expression after 7 days of infection. Ad-*TES2* effects compared with Ad-GFP at various MOI and times after transfection. Western blot shows TES expression only in cell lysates from Ad-*TES2*-infected cells. *B,* MCF-7 cells were used as control because the expression of *TES* is normal. No difference between Ad-*TES2* and Ad-GFP at various MOI was found. MCF-7 cells did not show expression of pro-caspase-3 (data not shown) because they do not constitutively express caspase-3. *C,* MES-SA cells: Ad-*TES2* infection of these cells for 9 days results in no caspase-activation but reduced survivin protein levels and overexpression of AIF. Western blot for TES protein shows TES expression only in cell lysates from Ad-*TES2*-infected cells. All of these data are obtained from two independent experiments in duplicate.

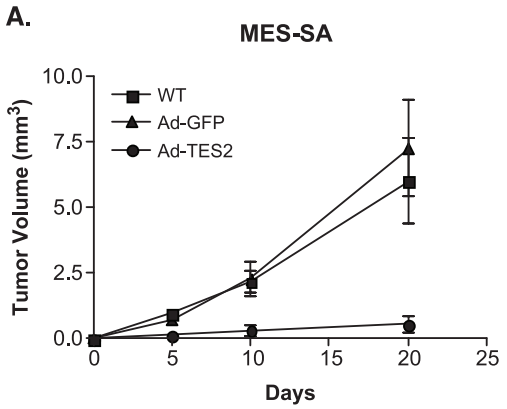

MES-SA	TUMOR INCIDENCE (%)	TUMOR WEIGHT(g) ± SD
WT	16/16 (100%)	0.405 ± 0.475
Ad-GFP	10/12 (83%)	0.399 ± 0.436
Ad-TES2	3/12 (25%)	0.0275 ± 0.057

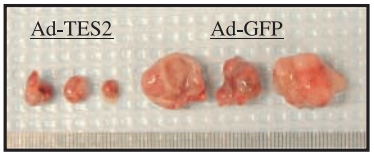

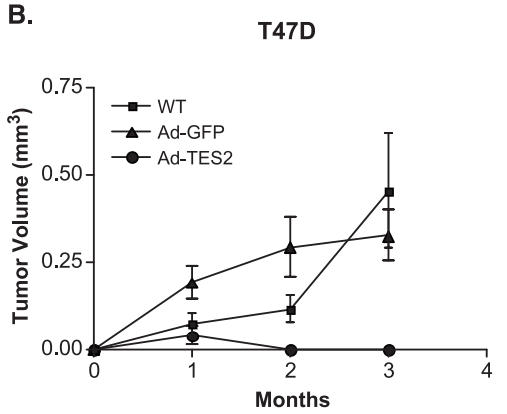

T47D	TUMOR INCIDENCE (%)	TUMOR WEIGHT(g) ± SD
WT	8/9 (88%)	0.013 ± 0.006
Ad-GFP	9/11 (81%)	0.014 ± 0.010
Ad-TES2	1/6 (16%)	0.001 ± 0.003

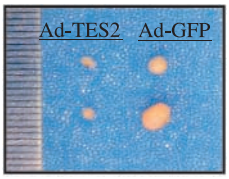

Fig. 5 Effects of *TES* expression on the tumorigenicity of Ad-*TES2*-transduced MES-SA (*A*) and T47D (*B*) cells in nude mice. *Left, in vivo* growth curves; *right,* tumor incidence, tumor weight (presented as average tumor weight with SD for each group of mice), and tumor formation in nude mice. MES-SA viable cells (3×10^6) have been infected *in vitro* at MOI 100 with Ad-*TES2* or with Ad-GFP (12 mice) or mock (16 mice) and cultured for 48 hours before s.c. injections in nude mice (*top right*). T47D viable cells (5×10^6) have been infected at MOI 100 with Ad-*TES2* (6 mice) or with Ad-GFP (11 mice) or mock (9 mice) and cultured for 48 hours before s.c. injections in nude mice (*bottom right*). As controls, we used wild-type (untreated) cells and Ad-GFP-infected cells. Animal studies were done twice.

The mechanism of tumor suppression by *TES* is not fully understood. TES protein contains three LIM domains in the COOH-terminal portion, which are crucial zinc finger structures working as protein-protein interaction motifs involved in both intramolecular and intermolecular interactions (21). In addition, LIM domains are found in various families of proteins, such as transcription factors, kinases, and cytoskeleton-associated proteins (21). TES protein also contains a PET domain in its NH_2-terminal region that probably plays a critical role for targeting TES to actin stress fibers (7). The human TES protein has extensive similarity to zyxin in both sequence and domain organization (20). Zyxin, widely expressed in human tissues, is a protein that may function in both signaling and architectural capacity in conjunction with actin cytoskeleton (22). A recent study confirms that transfected *TES* negatively regulates proliferation of T47D human invasive ductal breast carcinoma cells (20) and that TES is a component of focal adhesions and functions in events related to cell motility and adhesion (20). We found that after Ad-*TES2* transduction T47D cell line exhibited caspase-dependent apoptosis, whereas MES-SA cells showed a significant alteration at flow cytometry analysis and DNA fragmentation, but the pathway of cell death was independent of caspase activation. In T47D cells, we observed activation of both main proapoptotic caspase cascades, mitochondrial-mediated caspase-3 activation through caspase-9 (intrinsic pathway) and caspase-3 activation by caspase-8 (extrinsic pathway). In MES-SA cells, we observed down-regulation of survivin and overexpression of AIF without cytochrome *c* release and poly(ADP-ribose)polymerase cleavage. These data confirm a caspase-independent apoptosis that has been described in other studies (14, 15, 23). Survivin, a member of inhibitor of apoptosis proteins family, is expressed during development and absent or down-regulated in most normal tissues, but it is reexpressed in most cancers and associated with tumor aggression and decreased patient survival (16). Thus, the role of survivin in cell division has been coopted by the tumor cell to aid in its survival (14). AIF, instead, is a mitochondrion-localized flavoprotein with NADH oxidase activity that is encoded by a nuclear gene and it has been shown to translocate from mitochondria to the cytosol as well as the nucleus when apoptosis is induced. Mitochondrion-localized AIF is thought to be inert, as far as apoptosis modulation is concerned. In contrast, extramitochondrial AIF

causes cell death. AIF is believed to mediate caspase-independent death because inhibition of caspase activation or caspase activity does not abolish the proapoptotic action of this protein (24). Moreover, an antagonistic relationship between survivin and AIF provides further justification for the broad expression of survivin in cancers. It is possible that AIF translocation and caspase-independent apoptosis may represent a backup apoptotic mechanism in normal cells when caspases fail or become dysregulated. Tumor expression of survivin may confer suppression of AIF activity and eliminate this backup mechanism, thus further enhancing apoptotic resistance (16). All of these data suggest the possibility that overexpression of *TES* is associated with alterations of cell adhesion and motility resulting in the activation of various apoptosis mechanisms caspase dependent or caspase independent.

In conclusion, adenoviral infection with *TES* in cell lines not expressing the protein is followed by the induction of apoptosis *in vitro* and suppression of tumorigenicity *in vivo*, confirming the proposed role of *TES* as a tumor suppressor and suggesting future possibilities of its use in gene therapy.

REFERENCES

1. Tatarelli C, Linnenbach A, Mimori K, Croce CM. Characterization of the human *TESTIN* gene localized in the FRA7G region at 7q31.2. Genomics 2000;68:1–12.

2. Tobias ES, Hurlstone AFL, MacKenzie E, McFarlane R, Black DM. The *TES* gene at 7q31.1 is methylated in tumours and encodes a novel growth-suppressing LIM domain protein. Oncogene 2001;20:2844–53.

3. Huang H, Qian C, Jenkins RB, Smith DI. Fish mapping of YAC clones at human chromosomal band 7q31.2: identification of YACs spanning FRA7G within the common region of LOH in breast and prostate cancer. Genes Chromosomes Cancer 1998;21:152–9.

4. Razani B, Schlegel A, Liu J, Lisanti MP. Caveolin-I, a putative tumour suppressor. Biochem Soc Trans 2001;29:494–9.

5. Engelman JA, Zhang XL, Lisanti MP. Genes encoding human caveolin-1 and -2 are co-localized to the D7S522 locus (7q31.1), a known fragile site (FRA7G) that is frequently deleted in human cancers. FEBS Lett 1998;436:403–10.

6. Lin JC, Scherer SW, Tougas L, et al. Detailed deletion mapping with a refined physical map of 7q31 localizes a putative tumor suppressor gene for breast cancer in the region of MET. Oncogene 1996;13:2001–8.

7. Coutts AS, MacKenzie E, Griffith E, Black DM. TES is a novel focal adhesion protein with a role in cell spreading. J Cell Sci 2003; 116:897–906.

8. Ausubel FM, Brent R, Kingston M, et al. Analysis of proteins. In: Current protocols in molecular biology. New York: Wiley-Interscience, 1989. p. 10.1–10.20.

9. Aqeilan R, Yarkoni S, Lorberboum-Galski H. Interleukin 2-Bax: a novel prototype of human chimeric proteins for targeted therapy. FEBS Lett 1999;457:271–6.

10. Madsen M, Briand P. Relationship between tumorigenicity, *in vitro* invasiveness, and plasminogen activator production of human breast cell lines. Cancer 1990;26:793–7.

11. Tegeder I, Grosch S, Schmidtko P, et al. Protein-independent G_1 cell cycle block and apoptosis with morphine in adenocarcinoma cells: involvement of p53 phosphorylation. Cancer Res 2003;63: 1846–52.

12. Janicke RU, Sprengart ML, Wati MR, Porter AG. Caspase-3 is required for DNA fragmentation and morphological changes associated with apoptosis. J Biol Chem 1998;273:9357–60.

13. Liang Y, Yan C, Schor NF. Apoptosis in the absence of caspase-3. Oncogene 2001;20:6570–8.

14. Shankar SL, Mani S, O'Guin KN, Kandimalla ER, Agrawal S, Shafit-Zagardo B. Survivin inhibition induces human neural tumor cell death through caspase-independent and -dependent pathways. J Neurochem 2001;79:426–36.

15. Ahn HJ, Kim YS, Kim JU, Han SM, Shin JW, Yang HO. Mechanism of taxol-induced apoptosis in human SKOV3 ovarian carcinoma cells. J Cell Biochem 2004;91:1043–52.

16. Liu T, Brouha B, Grossman D. Rapid induction of mitochondrial events and caspase-independent apoptosis in Survivin-targeted melanoma cells. Oncogene 2004;23:39–48.

17. Couch FJ, Weber BL. Breast cancer. In: Vogelstein B, Kinzler KW, editors. The genetic basis of human cancer. New York: McGraw-Hill; 1998. p. 537–63.

18. Chauveinc L, Deniaud E, Plancher C, et al. Uterine sarcomas: the Curie Institut experience. Prognosis factors and adjuvant treatments. Gynecol Oncol 1999;72:232–7.

19. Le T. Adjuvant pelvic radiotherapy for uterine carcinosarcoma in a high risk population. Eur J Surg Oncol 2001;27:282–5.

20. Garvalov BK, Higging TE, Sutherland JD, et al. The conformational state of TES regulates its zyxin-dependent recruitment to focal adhesions. J Cell Biol 2003;161:33–9.

21. Bach I. The LIM domain: regulation by association. Mech Dev 2000;91:5–17.

22. Macalma T, Otte J, Hensler ME, et al. Molecular characterization of human zyxin. J Biol Chem 1996;271:31470–8.

23. van Gurp M, Festjens N, van Loo G, Saelens X, Vandenabeele P. Mitochondrial intermembrane proteins in cell death. Biochem Biophys Res Commun 2003;304:487–97.

24. Candè C, Vahsen N, Garrido C, Kroemer G. Apoptosis-inducing factor (AIF): caspase-independent after all. Cell Death Differ 2004;11: 591–5.

Clinical Cancer Research

Adenoviral Transduction of *TESTIN* Gene into Breast and Uterine Cancer Cell Lines Promotes Apoptosis and Tumor Reduction *In vivo*

Manuela Sarti, Cinzia Sevignani, George A. Calin, et al.

Clin Cancer Res 2005;11:806-813.